*J. Mol. Model.* **2000**, *6*, 166 – 170

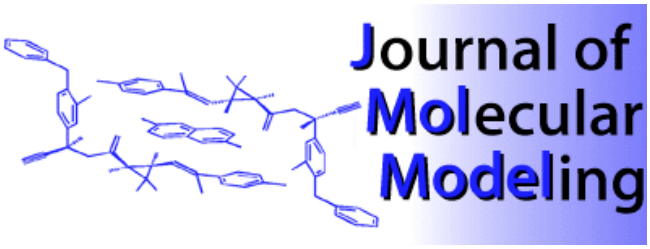


**FULL PAPER**



# Structure and Reactivity of Chiral Fenchone Based Organozinc Catalysts

**Bernd Goldfuss and Melanie Steigelmann**

Organisch-Chemisches Institut der Universität Heidelberg, Im Neuenheimer Feld 270, D-69120 Heidelberg, Germany.
E-mail: Bernd.Goldfuss@urz.uni-heidelberg.de

*Received: 28 July 1999/ Accepted: 8 December 1999/ Published: 28 February 2000*

**Abstract** The propensity of zinc alkoxides to dimerize arises from the polarity of $Zn^{(\delta+)}$-$O^{(\delta-)}$ units, which can be visualized by electrostatic potential plots, e. g. of the zinc chelate complex {methylzinc(1*R*,2*R*,4*S*)-2-*endo*-oxido-2-*exo*-(2-methoxyphenyl)-1,3,3-trimethylbicyclo[2.2.1] heptane}. Monomer-dimer equilibria of this fenchone-based methylzinc chelate complex and its derivatives determine catalyst reactivity in dialkylzinc additions to aldehydes and were computed [ONIOM (RHF/LanL2DZ:UFF)] to assess the relative reactivities of the catalysts. Increased monomer formation, i. e. increased catalyst reactivity, is predicted in ligand systems with bulky *t*-butyl and $Si(CH_3)_3$ *ortho*-substituents but not for the methyl derivative. Geometrical aspects of dimeric zinc chelate complexes, such as interring $C_{aryl}$-$C_{aryl}$ distances, the dimer forming and internal Zn-O bond distances and the $(H_3C)$-O-$C_{aryl}$-$C_{aryl}$ dihedral angles were found to correspond with the relative stabilities of the dimeric complexes. These geometrical criteria are promising structural probes to assess catalyst reactivity and hence are helpful tools for a rational catalyst design.

**Keywords** Catalyst design, Zinc alkoxides, Zinc complexes, ONIOM computations, Structure-reactivity relationships

## Introduction

The design of efficient chiral promoters for enantioselective 1,2-additions of organometallic reagents to prochiral carbonyl compounds is eminent in modern organic chemistry,[1] and organozinc complexes are highly promising catalysts.[2] Noyori et al. reported detailed experimental[3] and computational[4] studies of DAIB [(2*S*)-3-*exo*-(dimethylamino)isoborneol, Scheme 1] catalyzed dialkylzinc, $ZnR_2$ (R=Me, Et), additions to benzaldehyde.

The enantioselective step was found to proceed through "*anti*" and "*syn*" $\mu$-O-transition structures (Scheme 2). We have recently shown that $\mu$-O-transition structure models can be successfully employed to understand enantioselectivities with other chiral $\beta$-aminoalcohols, e. g., proline and 1,2-diphenylethane derivatives.[5]

Extensive studies by Noyori et al. have identified *monomeric* zinc chelate complexes as catalysts in DAIB-promoted dialkylzinc additions to aldehydes, while the *dimeric* catalysts are unreactive.[6] The equilibrium between monomeric and dimeric zinc chelate complexes (Scheme 1) was found to be crucial for the reactivity of the catalysts

*Correspondence to:* B. Goldfuss

*Dedicated to Professor Paul von Ragué Schleyer on the occasion of his 70th birthday*

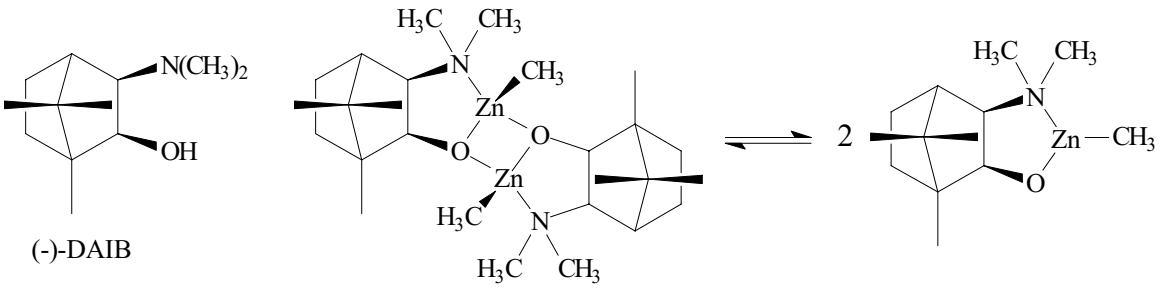


**Scheme 1** *Noyori's DAIB, 3-*exo*-(dimethylamino)isonorborneol, ligand and the dimer-monomer equilibrium of homochiral zinc chelate complexes*

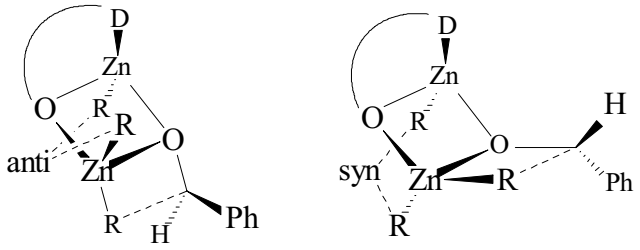


**Scheme 2** *"*μ-Anti*" and "*μ-syn*" transition structures, O∪D= chelating ligand. Anti and syn alignments of passive alkyl groups at Zn are shown.*

and provides the basis for chirality amplification phenomena.[6d-f, 7]

A huge number of chiral chelating ligands has been synthesized and applied in enantioselective additions of organozinc reagents to aldehydes,[2] but ligands with short synthetic routes are still desirable. An efficient one step addition of *ortho*-lithioanisole to (-)-fenchone yields the chiral chelating ligand **1** (Scheme 3). We have recently reported the X-ray crystal structure (Figure 1) of the dimeric chiral methyl zinc chelate complex of **1**, {methylzinc(1*R*,2*R*,4*S*)-2-*endo*-oxido-2-*exo*-(2-methoxyphenyl)-1,3,3-trimethylbicyclo[2.2.1] heptane}$_2$ (**2**)$_2$, which shows striking similarities with Noyori's DAIB based catalyst (Scheme 1).[8]

We here present a molecular modeling study (ONIOM, [9] RHF/LANL2DZ[10] : UFF[11]) on monomeric and dimeric **2** as well as its derivatives. Based on these computations we analyze relationships between geometrical details and relative reactivities of the complexes. Our study should provide helpful tools for a rational catalyst design in alkylzinc additions to aldehydes.

## Results and discussion

Our modular approach to chiral chelating ligand systems allows the efficient introduction of *ortho*-substituents (El) to modify both catalyst reactivity and selectivity,[12] as demonstrated in Scheme 3.

The O-Zn polarity in **2** provides the basis for its dimerization to (**2**)$_2$ (Figure 1). The polarity of the $O^{\delta-}$-$Zn^{\delta+}$ unit in **2** can be visualized by an electrostatic potential plot, showing red ($\delta^-$) and blue ($\delta^+$) areas at O and Zn, respectively (Figure 2).[13]

To predict relative reactivities of **2** and its derivatives as catalysts in dialkylzinc additions to aldehydes and to select the most promising catalyst, monomer-dimer equilibria were computed for each species with El= H (**2**), $CH_3$ (**2-Me**), $C(CH_3)_3$ (**2-Bu**) and $Si(CH_3)_3$ (**2-Si**) (Scheme 4). The stronger the equilibrium shifts towards the monomer, the higher is the predicted reactivity of the catalyst.

Morokuma's ONIOM method,[9] implemented in GAUSSIAN 98[14] was used for geometry optimizations and frequency computations. The inner core of the complexes was computed *ab initio* (RHF/LanL2DZ) while for the rest of the structure Rappé's universal force field (UFF)[11] was employed (Scheme 5). Hydrogen atoms were used to saturate the valences between the layers.

According to the computed equilibria (Table 1, Scheme 4), the least stable dimer is formed by **2-Bu**, followed by **2-Si**. Complexes **2** and **2-Me** give rise to more stable dimers

**Scheme 3** *Synthesis of chiral chelating ligands and methylzinc complexes*

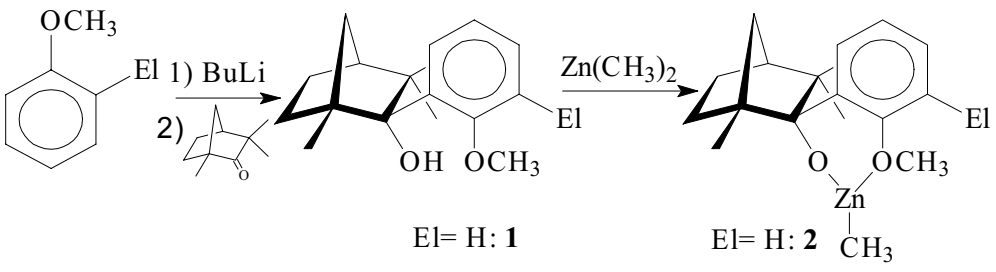

**Table 1** *Total (a.u.) and relative (kcal·mol$^{-1}$) energies of monomeric and dimeric zinc chelate complexes, ONIOM (RHF/LanL2DZ:UFF), Scheme 5 [a]*

| | monomer | dimer | rel.[b] |
|---|---|---|---|
| **2** | -178.38746 (273.4) | -356.82767 (551.2) | **-33.1** (-28.7) |
| **2-Me** | -178.37597 (291.2) | -356.80727 (588.1) | **-34.7** (-29.0) |
| **2-Bu** | -178.34885 (345.9) | -356.71862 (703.7) | **-13.1** (-1.2) |
| **2-Si** | -178.38075 (337.4) | -356.79500 (684.4) | **-21.0** (-11.4) |

*[a] Zero point energies (ZPE, unscaled, kcal·mol$^{-1}$) and ZPE corrected relative energies are given in parentheses. All computed structures were fully optimized and characterized by frequency computations as minima*

*[b] Relative energies of monomers and dimers are computed according to Scheme 4, negative energies correspond to exothermic dimerizations.*

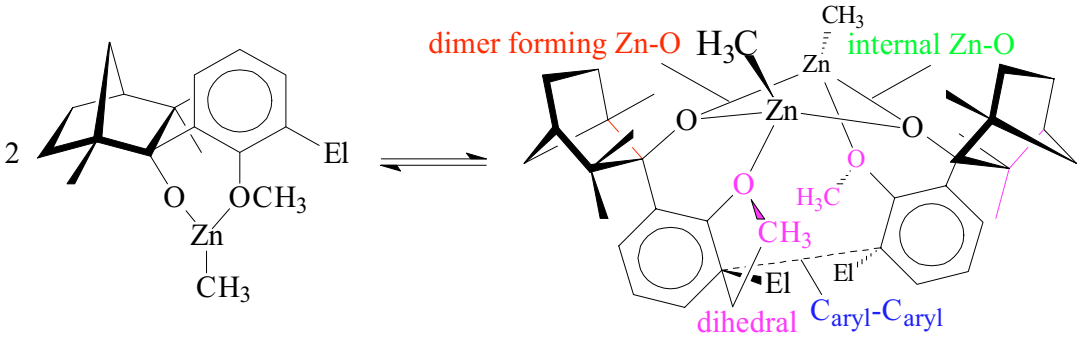


**Scheme 4** *Monomer-dimer equilibrium for zinc chelate complexes. El = H:* ***2*** *(**2**)$_2$; El = Me:* ***2-Me*** *(**2-Me**)$_2$; El = t-Bu:* ***2-Bu*** *(**2-Bu**)$_2$; El = SiMe$_3$:**2-Si** (**2-Si**)$_2$*

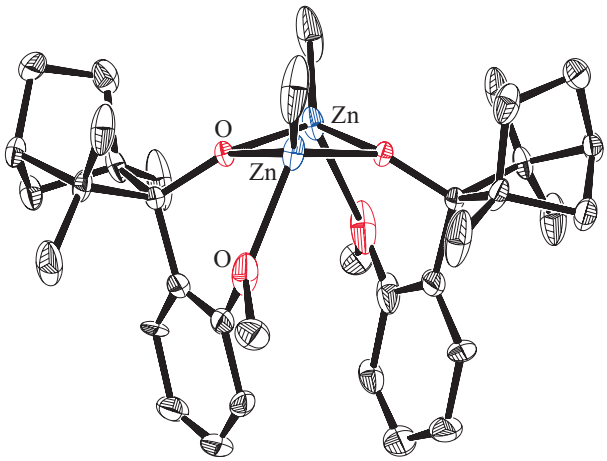


**Figure 1** *X-ray crystal structure of (**2**)$_2$. Hydrogen atoms are omitted for clarity [8]*

and hence are less reactive catalysts (Table 1). Which structural effects parallel the lower dimer stability of **2-Bu** and **2-Si** relative to **2** and **2-Me**?

A potential dimer stabilizing factor arises from π-stacking of the two phenylene moieties, as is evident in the X-ray crystal structure of (**2**)$_2$ (Figure 1). Shortest interring $C_{aryl}$-$C_{aryl}$ distances are apparent between $C_{(H)}$ atoms in *ortho*-position relative to the methoxy groups (3.50 Å, Table 2, Scheme 4). Only slightly longer $C_{aryl}$-$C_{aryl}$ distances are computed for (**2**)$_2$ and its methyl derivative (**2-Me**)$_2$. However, trimethylsilyl and *t*-butyl substitution in (**2-Si**)$_2$ and (**2-Bu**)$_2$ strongly increase the interring $C_{aryl}$-$C_{aryl}$ distances and hence destabilize the dimeric structures. The largest interring $C_{aryl}$-$C_{aryl}$ distance is computed for (**2-Bu**)$_2$, which also exhibits the lowest stability (Scheme 4).

Bond distances in the central $Zn_2O_2$ rings of the dimeric structures correspond to the lower stabilities of (**2-Bu**)$_2$ and (**2-Si**)$_2$ relative to (**2**) and (**2-Me**)$_2$. The *dimer forming* Zn-O distances are significantly shorter in the unsubstituted and methyl substituted species than for (**2-Bu**)$_2$ and (**2-Si**)$_2$ (Table 2, Scheme 4). In contrast, *internal* Zn-O distances are much shorter for the less stable dimers (**2-Bu**)$_2$ and (**2-Si**)$_2$ than for the more stable species (Table 2, Scheme 4). The longest *dimer forming* and the shortest *internal* Zn-O distance are apparent in the most unstable complex (**2-Bu**)$_2$.

**Table 2** *Geometrical details for the X-ray crystal structure of (**2**)$_2$[a] and computed dimers (Scheme 4)*

| | interring $C_{aryl}$-$C_{aryl}$ (Å) | Zn-$O_{dim.}$ (Å) | Zn-$O_{int.}$ (Å) | ($H_3C$)-O-$C_{aryl}$-$C_{aryl}$ dihedral (deg.) |
|---|---|---|---|---|
| **X-ray** (**2**)$_2$ [a] | 3.50 | 2.01 | 1.97 | -31.9 |
| (**2**)$_2$ | 3.85 | 2.14 | 1.91 | -50.2 |
| (**2-Me**)$_2$ | 3.66 | 2.15 | 1.91 | -58.1 |
| (**2-Bu**)$_2$ | 4.46 | 2.24 | 1.88 | -65.8 |
| (**2-Si**)$_2$ | 4.36 | 2.21 | 1.88 | -65.5 |

*[a] Due to disorder of $C_{aryl}$ and methoxy groups in the X-ray crystal structure of (**2**)$_2$, mean values were used to assess distances and angles*

**Scheme 5** *ONIOM (RHF/LanL2DZ:UFF) computations on monomeric and dimeric methyl zinc complexes*

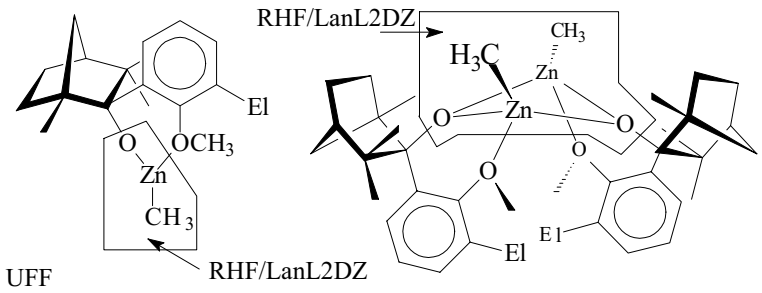


The ($H_3C$)-O-$C_{aryl}$-$C_{aryl}$ dihedral angle (Scheme 4), i. e. the tilt of the methoxy groups out of the aryl planes,[15] is an other geometrical measure for the stability of dimeric chelate complexes. The methoxy groups tilt significantly more out of the aryl planes for the bulky trimethylsilyl and *t*-butyl substituents in (**2-Si**)$_2$ and (**2-Bu**)$_2$ than for the methyl or unsubstituted species (**2-Me**)$_2$ and (**2**)$_2$ (Table 2). As the $C_{aryl}$-Si bond is longer than the $C_{aryl}$-C bond, the trimethylsilyl moiety is situated more remote than the *t*-butyl group and effects less the methoxy orientation. Hence, the largest deviation from methoxy-aryl coplanarity is found for (**2-Bu**)$_2$.

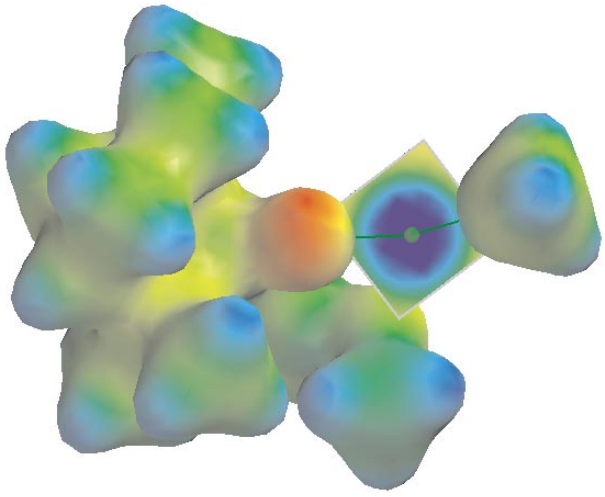

**Figure 2** *Electrostatic potential plot of **2**, showing $\delta^-$ (red at O) and $\delta^+$ (blue at Zn) areas, respectively*

## Conclusions

Our computational analyses of monomer-dimer equilibria of fenchone-based methylzinc chelate complexes predict increased monomer formation for bulky *t*-butyl (**2-Bu**) and $Si(CH_3)_3$ (**2-Si**) substituents in the *ortho*-position of **2**. This higher preference of monomers predicts an increased catalyst reactivity of **2-Si** and **2-Bu** in dialkylzinc additions to aldehydes relative to **2**. These monomer-dimer equilibria as measure of reactivity correspond to geometrical aspects of dimeric zinc chelate complexes, such as interring $C_{aryl}$-$C_{aryl}$ distances, the dimer forming and internal Zn-O bond distances and the ($H_3C$)-O-$C_{aryl}$-$C_{aryl}$ dihedral angles. These geometrical criteria are promising structural probes to assess catalyst reactivity from molecular groundstate structures.

**Acknowledgment** B. G. thanks the Fonds der Chemischen Industrie for a Liebig grant, the Deutsche Forschungsgemeinschaft and the Research Pool Foundation (University Heidelberg) for financial support and the Degussa-Hüls AG for generous gifts of chemicals. We are especially grateful to Prof. Dr. P. Hofmann for his generous support at Heidelberg.

**Supplementary material available** XYZ coordinates of computed zinc chelate complexes.

## References


1. (a) Thompson, A.; Corley, E. G.; Huntington, M. F.; Grabowski, E. J. J.; Remenar, J. F.; Collum, D. B. *J. Am. Chem. Soc.* **1998**, *120*, 2028. (b) Pierce, M. E.; Parsons, R. L. Jr., Radesca, L. A.; Lo, Y. S.; Silverman, S.; Moore, J. R.; Islam, Q.; Choudhury, A.; Fortunak, J. M. D.; Nguyen, D.; Luo, C.; Morgan, S. J.; Davis, W. P.; Confalone, P. N.; Chen, C.; Tillyer, R. D.; Frey, L.; Tan, L.; Xu, F.; Zhao, D.; Thompson, A. S.; Corley, E. G.; Grabowski, E. J. J.; Reamer, R.; Reider, P. J. *J. Org. Chem.* **1998**, *63*, 8536.
2. (a) Soai, K.; Niwa, S. *Chem. Rev.* **1992**, *92*, 833. (b) Noyori, R.; Kitamura, M. *Angew. Chem.* **1991**, *103*, 34; *Angew. Chem. Int. Ed. Engl.* **1991**, *30*, 49. (c) Evans, D. A. *Science* **1998**, *22*, 420.
3. (a) Kitamura, M.; Okada, S.; Suga, S.; Noyori, R. *J. Am. Chem. Soc.* **1989**, *111*, 4028. (b) Kitamura, M.; Suga, S.; Kawai, K.; Noyori, R. *J. Am. Chem. Soc.* **1986**, *108*, 6071.
4. (a) Yamakawa, M.; Noyori, R. *Organometallics* **1999**, *18*, 128. (b) Yamakawa, M.; Noyori, R. *J. Am. Chem. Soc.* **1995**, *117*, 6327.
5. Goldfuss, B.; Houk, K. N. *J. Org. Chem.* **1998**, *63*, 8998.
6. (a) Kitamura, M.; Okada, S.; Suga, S.; Noyori, R. *J. Am. Chem. Soc.* **1989**, *111*, 4028. (b) Kitamura, M.; Suga, S.; Niwa, M.; Noyori, R. *J. Am. Chem. Soc.* **1995**, *117*, 4832. (c) Yamakawa, M.; Noyori, R. *J. Am. Chem. Soc.* **1995**, *117*, 6327. (d) Kitamura, M.; Yamakawa, M.; Oka, H.; Suga, S.; Noyori, R. *Chem. Eur. J.* **1996**, *2*, 1173. (e) Kitamura, M.; Suga, S.; Oka, H.; Noyori, R. *J. Am. Chem. Soc.* **1998**, *120*, 9800. (f) Kitamura, M.; Oka, H.; Noyori, R. *Tetrahedron* **1999**, *55*, 3605.
7. Girard, C.; Kagan, H. B. *Angew. Chem.* **1998**, *110*, 3089; *Angew. Chem. Int. Ed. Engl.* **1998**, *37*, 2922.
8. Goldfuss, B.; Khan, S. I.; Houk, K. N. *Organometallics* **1999**, *18*, 2927.
9. Dapprich, S.; Komaromi, I.; Byun, K. S.; Morokuma, K.; Frisch, M. J. *THEOCHEM* **1999**, *461 - 462*, 1.
10. (a) Hay, P. J.; Wadt, W. R. *J. Chem. Phys.* **1985**, *82*, 270. (b) Wadt, W. R.; Hay, P. J. *J. Chem. Phys.* **1985**, *82*, 284. (c) Hay, P. J.; Wadt, W. R. *J. Chem. Phys.* **1985**, *82*, 299.
11. Rappé, A. K.; Casewit, C. J.; Colwell, K. S.; Goddard III, W. A.; Skiff, W. M. *J. Am. Chem. Soc.* **1992**, *114*, 10024.
12. Steigelmann, M. Diploma Thesis, University Heidelberg 1999.
13. PM3 optimized structure with electrostatic potential representations (surface and slice). PC-Spartan Pro, Wavefunction Inc., U.S.A. 1999.
14. Gaussian 98, Revision A.5; Frisch, M. J.; Trucks, G. W.; Schlegel, H. B.; Scuseria, G. E.; Robb, M. A.; Cheeseman, J. R.; Zakrzewski, V. G.; Montgomery, Jr., J. A.; Stratmann, R. E.; Burant, J. C.; Dapprich, S.; Millam, J. M.; Daniels, A. D.; Kudin, K. N.; Strain, M. C.; Farkas, O.; Tomasi, J.; Barone, V.; Cossi, M.; Cammi, R.; Mennucci, B.; Pomelli, C.; Adamo, C.; Clifford, S.; Ochterski, J.; Petersson, G. A.; Ayala, P. Y.; Cui, Q.; Morokuma, K.; Malick, D. K.; Rabuck, A. D.; Raghavachari, K.; Foresman, J. B.; Cioslowski, J.; Ortiz, J. V.; Stefanov, B. B.; Liu, G.; Liashenko, A.; Piskorz, P.; Komaromi, I.; Gomperts, R.; Martin, R. L.; Fox, D. J.; Keith, T.; Al-Laham, M. A.; Peng, C. Y.; Nanayakkara, A.; Gonzalez, C.; Challacombe, M.; Gill, P. M. W.; Johnson, B.; Chen, W.; Wong, M. W.; Andres, J. L.; Gonzalez, C.; Head-Gordon, M.; Replogle, E. S.; Pople, J. A. Gaussian, Inc., Pittsburgh PA, 1998.
15. Out of plane methoxy aryl moieties are also apparent in the X-ray crystal structure of a lithium (*o*-anisyl) silylamide: Goldfuss, B.; Schleyer, P. v. R.; Handschuh, S.; Hampel, F. *J. Organomet. Chem.* **1998**, *552*, 285.